PCCP

Accepted Manuscript

This is an *Accepted Manuscript*, which has been through the Royal Society of Chemistry peer review process and has been accepted for publication.

Accepted Manuscripts are published online shortly after acceptance, before technical editing, formatting and proof reading. Using this free service, authors can make their results available to the community, in citable form, before we publish the edited article. We will replace this *Accepted Manuscript* with the edited and formatted *Advance Article* as soon as it is available.

You can find more information about *Accepted Manuscripts* in the Information for Authors.

Please note that technical editing may introduce minor changes to the text and/or graphics, which may alter content. The journal's standard Terms & Conditions and the Ethical guidelines still apply. In no event shall the Royal Society of Chemistry be held responsible for any errors or omissions in this *Accepted Manuscript* or any consequences arising from the use of any information it contains.

ROYAL SOCIETY OF CHEMISTRY

www.rsc.org/pccp

Chemical Science

RSCPublishing

ARTICLE

Tuning the Singlet-Triplet Energy Gap of AIE Luminogens: Crystallization-Induced Room Temperature Phosphorescence and Delay Fluorescence, Tunable Temperature Response, Highly Efficient Non-doped Organic Light-Emitting Diodes

Cite this: DOI: 10.1039/x0xx00000x

Received 00th January 2012,
Accepted 00th January 2012

DOI: 10.1039/x0xx00000x

www.rsc.org/

Jie Li,[a] Yibin Jiang,[b] Juan Cheng,[c] Yilin Zhang,[c] Huimin Su,[c] Jacky W. Y. Lam,[a] Herman H. Y. Sung,[a] Kam Sing Wong,[c] Hoi Sing Kwok,[b] and Ben Zhong Tang*[ade]

In this contribution, we finely tuned the singlet-triplet energy gap ($\triangle E_{ST}$) of AIE-active materials to modulate their fluorescence, phosphorescence and delay fluorescence via rational molecular design and investigated the possible ways to harvest their triplet energy in OLEDs. Noteworthy, two molecules *o*-TPA-3TPE-*o*-PhCN and *o*-TPA-3TPE-*p*-PhCN with larger $\triangle E_{ST}$ values (0.59 eV and 0.45 eV, respectively) emitted efficient long-lived low temperature phosphorescence in their glassy solutions and exhibited efficient crystallization-induced room temperature phosphorescence (RTP). Meanwhile, it was the first time to observe a novel crystallization-induced delay fluorescence phenomenon in another AIE-active molecule *p*-TPA-3TPE-*p*-PhCN owing to its very small $\triangle E_{ST}$ value (0.21 eV). It was also found that molecules with various $\triangle E_{ST}$ values showed significantly different temperature sensitivity. Non-doped electroluminescent (EL) devices using these molecules as light-emitting layers were fabricated, exhibiting external quantum efficiencies (*EQE*) higher than theoretical values of purely singlet emitter type devices. Particularly, *p*-TPA-3TPE-*p*-PhCN showed outstanding device performances with high luminance and efficiencies up to 36900 cd/m^2, 11.2 lm/W, 12.8 cd/A and 4.37%, respectively, considering that its solid-state quantum yield was only 42%. All the above observations suggested that tuning the $\triangle E_{ST}$ values of AIE materials is a powerful methodology to generate many more interesting and meaningful optoelectronic properties.

Introduction

Utilization of triplet energy from organic luminescent materials is of great interest owing to their potential applications in display, solid-state lighting, optical storage and sensors, especially in OLED devices where singlet/triplet energy ratio is generally considered as 1 : 3.[1] Organometallic phosphorescent materials can readily contribute their triplet energy to successfully achieve the internal quantum efficiency of OLEDs up to unite thanks to their strong spin-orbital coupling and very short triplet-state lifetime, when doped into the rigid matrix with high triplet energy levels.[2] While for purely organic materials, it is rather difficult to directly harvest their triplet energy in EL devices due to the very weak spin-orbital coupling and much longer triplet-state lifetime which make it easily consumed by rapid nonradiative vibrational relaxation.[3]

Several reports utilized different strategies to achieve efficient RTP from purely organic luminogens. Tang et al. observed RTP from crystals of benzophenone and its halogenated derivatives due to the minimized vibrational relaxation and enhanced spin-orbital coupling by the heavy atom effect.[4] Similarly, Bolton et al. developed color-tunable organic phosphorescence materials by implementing a directed heavy atom effect with halogen atoms in the crystalline systems.[5] Lee et al. reported bright RTP with 7.5% phosphorescence quantum yield by embedding a purely organic phosphor into amorphous glassy isotactic poly(methyl methacrylate) matrix with reduced beta (β)-relaxation.[6] Hirata et al. achieved efficient persistent RGB RTP with a quantum yield > 10% and a lifetime > 1 s in air utilizing organic host-guest materials and molecular design to minimize the non-radiative deactivation pathway of triplet excitons.[7] However, no sucess has been achived by directly harvesting

Physical Chemistry Chemical Physics Accepted Manuscript

phosphorescence of these purely organic luminescnt materials in EL devices yet.

Recent impressive work by Adachi et al. paves a totally new direction to utilize triplet energy to fabricate highly efficient purely organic light emitting diodes via thermally activated delay fluorescence (TADF).[8] By rational HOMO/LUMO engineering, very small $\triangle E_{ST}$ values can be obtained by intramolecular charge transfer (ICT) within molecular systems containing spatially separated donor and acceptor moieties, then strong reverse intersystem crossing is achieved to promote delay fluorescence which can endow fluorescence-based EL devices efficiently promoting the triplet excitons back to singlet states. Based on this careful design, very high *EQE* of 19.3%, 11.2% and 8.0% are achieved in green, orange and red purely organic light emitting diodes, respectively, which are all much higher than those conventional fluorescence-based OLEDs.[8i] Smilar to the case of organometallic systems, these TADF molecules must be doped into rigid matrixes with high triplet energy levels for efficient triplet energy harvesting.

The extensively studied traditional fluorescent or phosphorescent organic dyes commonly suffer from the aggregation-caused quenching (ACQ) problem in the condensed phase, making their EL device structure more complex by doping the dyes in properly matched matrix.[9] On the contrary, luminescent materials with AIE characteristics, show dramatically enhanced light emission in the condensed phase, generating efficient OLEDs with much simpler non-doped device structures.[10] However, so far, all of these non-doped OLEDs can still only utilize the singlet excitons, without any progress on harvesting the triplet energy for more efficient performances yet.

In this contibution, efforts are devoted to novel molecular design to manipulate the fluorescence, phosphorescence and delay fluorescence behaviours of AIE-active materials, and exploration of possible ways to harvest triplet excitons in the non-doped OLED devices. A series of AIE-active triphenylethene (3TPE)-based chromophores (D-3TPE-A, Scheme 1) incorporated with TPA and PhCN as the electron donor and acceptor at different substituted positions, respectively, were synthesized in good yields. Their $\triangle E_{ST}$ values were finely controlled by HOMO/LUMO engineering and steric hindrance, resulting in rational modulation on their fluorescence, phosphorescence or delay fluorescence behaviors in 77K glassy solution or in the crystalline state, and their EL devices were constructed with much improved performances.

Results and discussion

Molecular Design and Synthesis

To control $\triangle E_{ST}$ values of AIE luminogens, the incorporation of electorn donor and acceptor into π conjugated systems to manipulate HOMO/LUMO distribution is widely used.[8] Herein the steric hindrance is also rationally designed to finely tune $\triangle E_{ST}$ values. According to these basic molecular design principles, a series of triphenylethene (3TPE)-based chromophores (D-3TPE-A, Scheme 1) incorporated with TPA and PhCN as electron donating and accepting groups at different substituted positions, respectively, were synthesized via a three-step route by using highly efficient Suzuki coupling and Wittig reaction (Scheme 2). All these four molecules possess exactly the same atoms but only with different functional group connecting sites (Synthesis details and structural characterizations are included in Supporting Information).

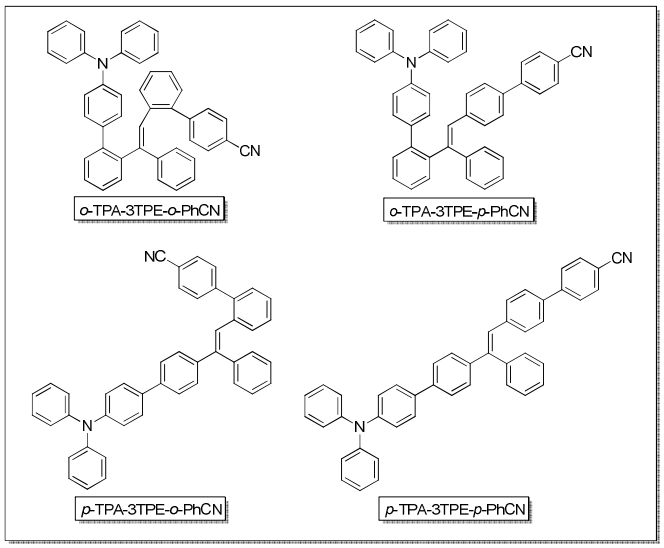

Scheme 1. Chemical structure of D-3TPE-A molecules

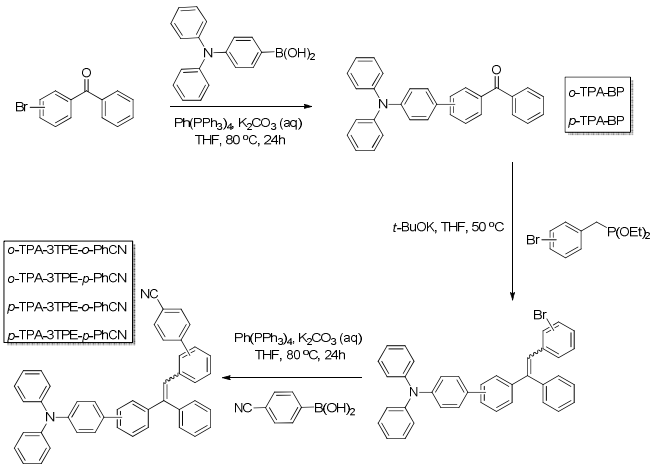

Scheme 2. General synthetic routes for D-3TPE-A molecules

Aggregation-Induced Emission & Twisted Intramolecular Charge Transfer (TICT)

Generally, the steric hindrance of *ortho*-substitutuents can twist the molecular conformation and reduce the conjugation significantly, thus widening the ground state energy gap as shown in the order of *p*-TPA-3TPE-*p*-PhCN < *p*-TPA-3TPE-*o*-PhCN < *o*-TPA-3TPE-*p*-PhCN < *o*-TPA-3TPE-*o*-PhCN (Table S1, Fig. S5). The emission of the molecules in THF solutions generally occurs at redder region than that in the film state due to the solvent polarity effect on the light emission process (Table S1, Fig. S6). It is found that molecules with cyano group at the *para*-position show redder emission, as demonstrated by the longer emission wavelength of *o*-TPA-3TPE-*p*-PhCN and *p*-TPA-3TPE-*p*-PhCN. Interestingly, *o*-TPA-3TPE-*o*-PhCN shows local excited (LE) state emission at 402 nm and ICT emission at 464 nm in the THF solution, while others only

Physical Chemistry Chemical Physics Accepted Manuscript

 This journal is © The Royal Society of Chemistry 2012

exhibit obvious ICT emission peak with LE emission as small shoulder at around 400 nm, indicating that the twisted conformation can interrupt the molecular conjugation and thus partially hamper the charge transfer process.

The PL spectra of D-3TPE-A molecules in THF/water mixtures with different water volume fractions and the associated plots of PL intensity versus the composition of the solvent mixtures are shown in Fig. 1 and Fig. S8. Generally, two similar trends are commonly observed in all the molecules: the intensity of the ICT emission peak is decreased at low water fractions but becomes higher upon further addition of water, the other one is that the ICT emission wavelength red shifts at the beginning and moves hypsochromically at high water fractions. Such phenomenon is quite common for AIE chromophores with donor and acceptor substituents, and can be well interpreted by the AIE and TICT mechanisms.[11]

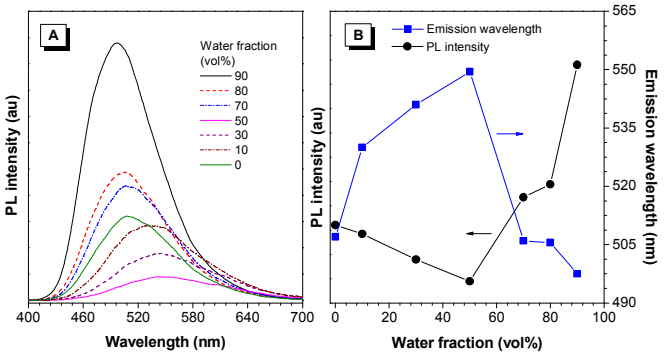

Fig. 1 (A) PL spectra of *p*-TPA-3TPE-*p*-PhCN in THF/water mixtures with different water fractions at room temperature, excitation wavelength: 350 nm, respectively. Dye concentration: 10 μM. (B) Plots of PL intensity and emission wavelength versus water fraction of *p*-TPA-3TPE-*p*-PhCN.

To further investigate the relationship between molecular structure and ICT effect, solvent effect on the fluorescence of D-3TPE-A molecules was detailedly studied (Fig. S9). Generally, these four molecules all show the positive solvatochromic behaviors, that is, their fluorescence emissions bathochromically shift with increasing solvent polarity. When changing the solvent from hexane to DMSO, their colors gradually red shift from blue to yellow or orange. Compared with *p*-TPA-*o*-PhCN and *p*-TPA-*p*-PhCN, which exhibit only 121 and 115 nm emission wavelength change, *o*-TPA-*o*-PhCN and *o*-TPA-*p*-PhCN show more pronounced solvatochromic effect with 137 and 144 nm shift, respectively, probably due to their highly twisted conformations, which allow a broader angular probability distribution.[12]

$\triangle E_{ST}$ and Low Temperature Phosphorescence

It is found that the glassy solid solution of D-3TPE-A molecules at 77 K exhibit strong fluorescence mixing with efficient phosphorescence. As shown by the fluorescent photographs in the inset of Fig. 2, under UV irradiation, the glassy solid solutions of all the four molecules emitted extremely intense photoluminescence, after removal of UV light, *p*-TPA-3TPE-*p*-PhCN glassy solid turned dark immediately while the other three still emitted intense green light. Then after 2s, 4s and 6s, the emission of *p*-TPA-3TPE-*o*-PhCN, *o*-TPA-3TPE-*p*-PhCN and *o*-TPA-3TPE-*o*-PhCN gradually turned off one after another, respectively. It is indicated that as the steric hindrance gradually increases, the phosphorescence lifetime prolongs correspondingly.

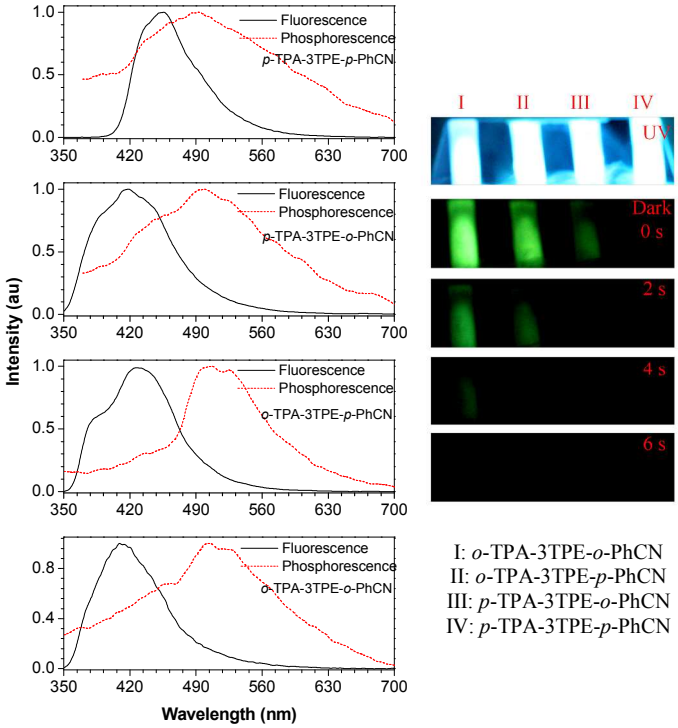

Fig. 2 Fluorescence and phosphorescence of D-3TPE-A molecules in n-hexane at 77 K. Dye concentration: 10 μM. Delay time: 1 ms. Inset: photographs of D-3TPE-A molecules in their glassy solid solutions at 77 K under UV excitation and after UV excitation, respectively. Dye concentration: 10 μM.

To further investigate the low temperature phosphorescence, prompt PL spectra (fluorescence) and 1-ms delay PL spectra (phosphorescence) of D-3TPE-A molecules in *n*-hexane solutions at 77 K were measured (Fig. 2) and $\triangle E_{ST}$ values were determined from the energy difference between the emission wavelengths of fluorescence and phosphorescence at 77 K as listed in Table S3. Interestingly, it was found that the phosphorescence peaks of the molecules with TPA moiety at the *ortho*-position were very similar, locating at around 510 nm, while for *p*-TPA-3TPE-*o*-PhCN and *p*-TPA-3TPE-*p*-PhCN, their phosphorescence peaks shifted to 495 nm. All the phosphorescence spectra were broad and structureless, indicating that their phosphorescence may originate from ^{3}CT states.[13] Noteworthily, the $\triangle E_{ST}$ value of *p*-TPA-3TPE-*p*-PhCN is very small as low as 0.21 eV owing to the lowered singlet energy level and the raised triplet energy level, while for other three molecules *o*-TPA-3TPE-*p*-PhCN, *p*-TPA-3TPE-*o*-

Physical Chemistry Chemical Physics Accepted Manuscript

PhCN and *o*-TPA-3TPE-*o*-PhCN, their $\triangle E_{ST}$ values are 0.45 eV, 0.45 eV and 0.59 eV, respectively, mostly due to the larger steric hindrance which can interrupt the conjugation and damatically blue shift their fluorescence.

What is the mechanism behind that steric hindrance can gradually prolong the low temperature phosphorescence lifetime of D-3TPE-A molecules? According to the Jablonski diagram, intersystem crossing (ISC) and reverse intersystem crossing (RISC) are the first photophysical processes that need to be considered for the investigation on phosphorescence. $\triangle E_{ST}$ is a key factor to determine the rate constant of ISC and RISC processes. The RISC rate constant (k_{RISC}) is generally estimated from $\exp(-\triangle E_{ST}/k_BT)$, where k_B is the Boltzmann constant and T is temperature. Therefore, k_{RISC} increases exponentially with the $\triangle E_{ST}$ value reducing. According to the above results, for D-3TPE-A molecules, with the steric hindrance increasing, the ΔE_{ST} values gradually become larger, thus their k_{RISC} values significantly decrease accordingly, resulting in greater triplet populations as well as longer phosphorescence lifetime, according to $\tau_{phos} = 1/(k_{nr} + k_{RISC} + k_r)$, wherenin k_{nr} and k_r are the rate constant of nonradiative and radiative decay, respectively. Especially for *p*-TPA-3TPE-*p*-PhCN with such a small $\triangle E_{ST}$ value as low as 0.21 eV, its low temperature phosphorescence lifetime is very short and cannot be detected by naked eyes.

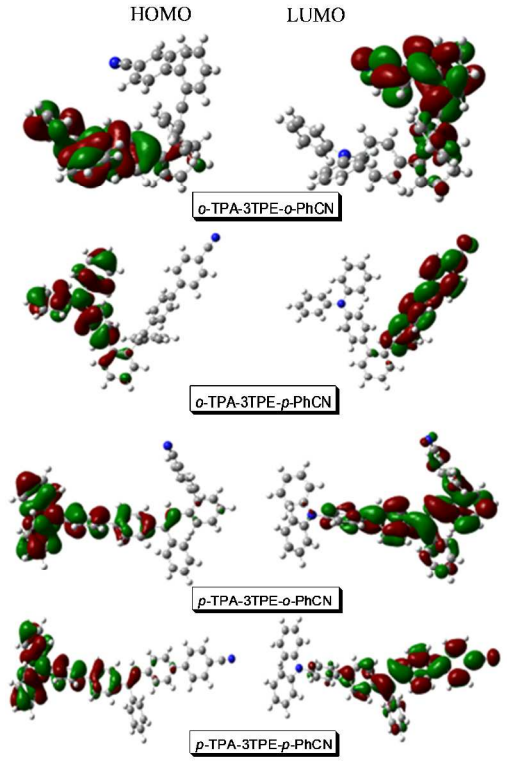

Fig. 3 Frontier MOs of D-3TPE-A molecules calculated with DFT at the B3LYP/6-31G(d) level by applying the Gaussian 09 program.

However, although *o*-TPA-3TPE-*p*-PhCN and *p*-TPA-3TPE-*o*-PhCN have almost the same $\triangle E_{ST}$ value (0.45 eV), *o*-TPA-3TPE-*p*-PhCN exhibits longer phosphorescence than *p*-TPA-3TPE-*o*-PhCN. To answer this question, density functional theory (DFT) calculations for D-3TPE-A molecules were carried out using a suite of Gaussian 09 program to study the frontier molecular orbital distribution. The nonlocal density functional of Beck's three-parameters employing Lee-Yang-Parr functional (B3LYP) with 6-31G (d) basis sets were used for the calculation. The molecular simulation results are shown in Fig. 3. For all of the four molecules, generally their HOMO are localized on the TPA group with similar HOMO energy level, while LUMO are distributed over the left part of the molecules. Complete HOMO/LUMO separation was observed in *o*-TPA-3TPE-*o*-PhCN with the largest steric hindrance due to the interruption of conjugation in triphenylethene core resulted from the highly twisted conformation (Fig. S11), also indicated by the relatively low quantum yield (16%, Table S1). *p*-Substituted position of the donor TPA can extend the LUMO and raise the LUMO energy level of *o*-TPA-3TPE-*p*-PhCN, while due to the high steric hindrance from the *o*-substituted TPA part, HOMO/LUMO separation is still well achieved, but with relatively higher conjugation than that in *o*-TPA-3TPE-*o*-PhCN, companying with higher quantum efficiency (32%, Table S1). HOMO/LUMO overlapping is observed in *p*-TPA-3TPE-*o*-PhCN and *p*-TPA-3TPE-*p*-PhCN owing to the smaller steric hindrance and relatively planar conformation, resulting higher quantum yield (40% and 42%, respectively, Table S1). Generally, the high steric hindrance can twist the 3TPE core, and thus affect the electron communication between the donor and acceptor even break the conjugation, accompanying with better HOMO/LUMO separation.

It is believed that the triplet states of D-3TPE-A molecules are mostly possibly promoted by the n-π^* transitions on the TPA moieties.[13,14] The partial HOMO/LUMO overlapping in *p*-TPA-3TPE-*o*-PhCN suggests that the electron communication between TPA and PhCN parts is more convenient, indicating that the n electron on the TPA can be much more delocalized to a larger π conjugated systems, while in *o*-TPA-3TPE-*p*-PhCN, n electrons are almost confined at the TPA part since the electron conmunication is poor between the electron donor and acceptor indicated by the complete localization of HOMO/LUMO in *o*-TPA-3TPE-*p*-PhCN. Therefore, the n-π^* transition in *p*-TPA-3TPE-*o*-PhCN will suffer from much more severe vibrational relaxation along the whole molecule, thus shortening its phosphorescence lifetime.

Crstallization-Induced Room Temperature Phosphorescence and Delay Fluorescence

Low temperature phosphorescence study suggests that the triplet states of D-3TPE-A molecules are optically allowed, so their RTP can be anticipated. Adequately suppressing vibrational relaxation is perhaps the most important and challenging aspect of achieving efficient purely organic RTP. So far RTP can be successfully achieved either via crystal

Physical Chemistry Chemical Physics Accepted Manuscript

This journal is © The Royal Society of Chemistry 2012

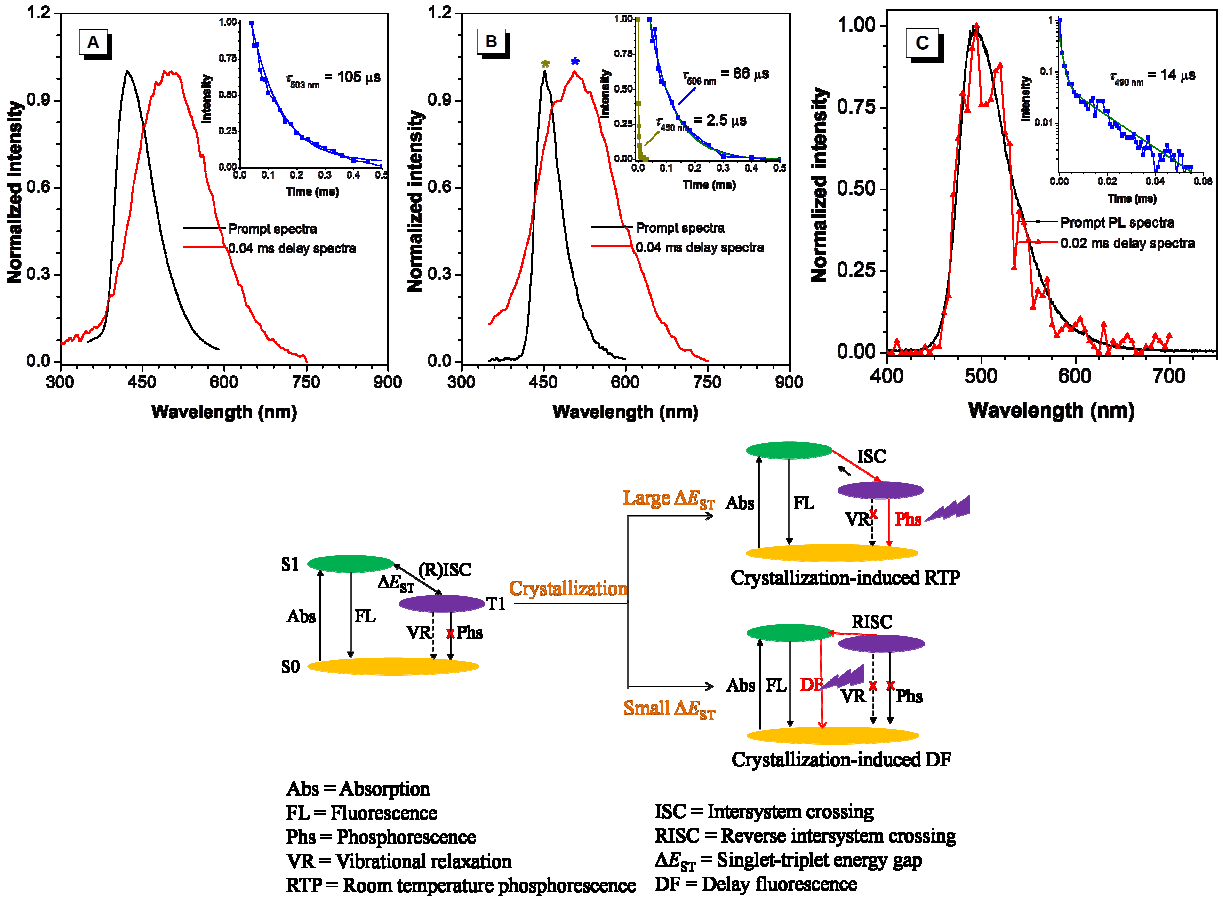

Fig. 4 Normalized prompt and delay PL spectra of the crystals of (A) *o*-TPA-3TPE-*o*-PhCN, (B) *o*-TPA-3TPE-*p*-PhCN and (C) *p*-TPA-3TPE-*p*-PhCN at room temperature. Inset: lifetime decay curves at (A) 503 nm, (B) 450 nm, 506 nm, and (C) 490 nm. (A) and (B, lifetime at 506 nm) were obtained by time window method using a Perkin-Elmer LS 55 spectrofluorometer, (B, lifetime time at 450 nm) and (C) was measured via a time-resolved fluorescence spectrometer with a 1-μs resolution. Inset scheme: mechanistic illustration about crystallization-induced phosphorescence and delay fluorescence.

engineering[4, 5] or by embedding in inert and rigid matrixes[6, 7] which can efficiently suppress the vibrational relaxation. Interestingly, RTP was readily detected in the crystalline state of *o*-TPA-3TPE-*p*-PhCN (microcrystals) and *o*-TPA-3TPE-*o*-PhCN (single crystals) with the triplet state emission locating at 506 nm and 503 nm after 0.04-ms delay, which was similar to those in their glassy solution at 77 K, although their strong fluorescence with rather sharp peaks at 452 nm and 422 nm still dominated (Fig. 4, S10 and Table S3). And the corresponding phosphorescence lifetime values are 86 μs and 105 μs, respectively, also indicating that larger $\triangle E_{ST}$ values can ensure longer phosphorescence lifetime.

Compared with those reported RTP from purely organic crystals via utilizing heavy atom effect such as bromine atom and carbonyl group to promote spin-orbital coupling,[4, 5] however, which is generally of no good for high photoluminescence efficiency, herein D-3TPE-A molecules have no suffer from heavy atom effect or no bother from doping processes. Therefore, crystallization of AIE-active materials with n-π^* transition and high $\triangle E_{ST}$ values via adequate molecular design provides an alternative promising approach to promote the purely organic phosphorescence.

As for the crystal of *p*-TPA-3TPE-*p*-PhCN (the crystal of *p*-TPA-3TPE-*o*-PhCN was not obtained), its 0.02-ms delay spectrum shares almost the same peak with the prompt spectrum at around 495 nm, with the delay time increasing, this peak only becomes weaker but without any wavelength shift (Fig. S10C), indicating that it should be attributed to the delay fluorescence. And its lifetime for the longer radiative decay is around 14 μs, confirming that it is delay fluorescence from this AIE-active crystal, which is extraordinary if not precedence. In the literature, delay fluorescence is usually generated by doping charge tranfer complexes with proper HOMO-LUMO balance or dyes with very small $\triangle E_{ST}$ values into rigid matrix with high triplet energy levels,[8] for one reason, those molecules generally suffer from ACQ problems in their solid states, another is that the triplet energy readily undergo non-radiative decay via vibrational relaxation. Meanwhile, a relatively long-lived radiative decay with the lifetime of about 2.5 μs was also detected at the 450 nm emission peak of *o*-TPA-3TPE-*p*-PhCN

Physical Chemistry Chemical Physics Accepted Manuscript

(inset in Fig. 4B), indicating partially delay fluorescence was obtained as well.

Herein we have got an feasible and simpler approach to promote delay fluorescence from the crystals of AIE-active molecules with small $\triangle E_{ST}$ values: the crystal structure can minimize the vibrational relaxation thus preserving the triplet energy at room temperature, while the small $\triangle E_{ST}$ promotes the phonons up convert from the triplet to the singlet, giving out delay fluorescence. Notewothy, *o*-TPA-3TPE-*p*-PhCN also shows some delay fluorescence due to a large overlap between fluorescence and phosphorescence spectra (Fig. 4), illustrating that with the $\triangle E_{ST}$ values decreasing, the possibility for the phonons to up convert from triplet to singlet states is increasing, which is a gradual change rather than a mutation process. This could be high potential for utilizing triplet excitons in non-doped OLEDs with exceptionally efficient performances, as aformentioned in the introduction.

$\triangle E_{ST}$ and Temperature Response

Generally the fluorescence of D-TPE-A molecules gradually decreased with increasing the temperature in the thin film (Fig. S13) due to the activated vibrational relaxation which can increase the non-radiative decay. Interestingly, it is found that the molecule with a smaller $\triangle E_{ST}$ value shows slower downward trend (Fig. 5). According to the above discussion, smaller $\triangle E_{ST}$ value promotes faster reverse intersystem crossing and elevated temperature can also enhance k_{RISC} according to the equation of $k_{RISC} \propto \exp(-\triangle E_{ST}/k_BT)$, thus more triplet phonons return to the single state. It should be realized that this fluorescence compansation is still not enough to make up the fluorescene lost upon heating, only giving out slower downward trend in Fig. 5, since this experiment was carried out in amorphous thin films where severe vibrational relaxation is prone to occur. Noteworthy, *o*-TPA-3TPE-*p*-PhCN and *p*-TPA-3TPE-*o*-PhCN share similar temperature sensitivity owing to their $\triangle E_{ST}$ of almost the same value. Anyway, it was demonstrated as an effective approach to manipulate the temperature responsibility of luminescent materials via controlling their $\triangle E_{ST}$ values.

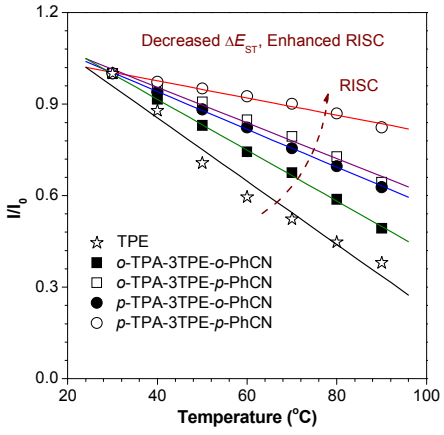

Fig. 5 Normalized intensity versus temperature curves of D-3TPE-A molecules and TPE (as reference) in the thin film.

Electroluminescence

Although the solid-state quantum yields of D-3TPE-A molecules are not high (only 23% ~ 42%) compared with other AIE-active chromophores,[10] their EL devices were fabricated to investigate the effect of $\triangle E_{ST}$ engineering on the EL performances and some results were pretty interesting. All the EL devices were fabricated in the same configuration of indium tin oxide (ITO)/NPB/X/TPBi/LiF/Al, where X = D-3TPE-A molecules, TPBi is 1,3,5-tris(N-phenylbenzimidazol-2-yl) benzene (the electron-transport layer) and NPB is 1,4-bis[(1-naphthylphenyl)amino]biphenyl (the hole-transport layer). As shown in Fig. S14, S15 and Table 1, generally *o*-TPA-3TPE-*o*-PhCN and *o*-TPA-3TPE-*p*-PhCN exhibited much poorer electroluminescent performances due to their bad conjugation induced by the large steric hindrance, for example, *o*-TPA-3TPE-*o*-PhCN possessed the worst luminance and efficiencies as low as 146 cd/m^2, 2.3 lm/W, 2.7 cd/A and 1.72%, respectively. And *o*-TPA-3TPE-*p*-PhCN/*p*-TPA-3TPE-*o*-PhCN showed better efficiencies with the values of 6.3/4.2 lm/W, 8.3/4.8 cd/A and 2.96/2.93%, but with relatively low luminance of 1090/3790 cd/m^2, respectively. Noteworthily, *p*-TPA-3TPE-*p*-PhCN, which possessed the best conjugation and lowest $\triangle E_{ST}$ value, exhibited extraordinary EL performance with pretty high luminance and efficiencies up to 36900 cd/m^2, 11.2 lm/W, 12.8 cd/A and 4.37%, respectively, considering that its solid-state quantum yield is only 42%.

Particularly, if only EQE_{max} was taken into consideration, it was found that all these four molecules showed very high conversion from PL efficiency to EL efficiency. Theoretically, according to the general assumptions of pure singlet emitter-based EL devices (singlet/triplet exciton ratio is 1:3, and the out coupling efficiency is 0.2 for the devices without optimizations), their calculated EQE_{max} values are only 1.2%, 1.6%, 2.0% and 2.1%, respectively. However, experimentally, their EQE_{max} values were 1.72%, 2.96%, 2.93% and 4.37%, respectively, which were all much higher than theoretical values.

Moreover, for *o*-TPA-3TPE-*p*-PhCN and *p*-TPA-3TPE-*p*-PhCN, their experimental EQE_{max} values are almost twice of the theoretical ones. As show in Fig. S14A, their EL emission peaks locate at 516 nm and 512 nm, both covering their triplet-state emission ranges, meanwhile considering the observation of crystallization-induced delay fluorescece aforementioned, one can expect that these two molecules can have some delay fluorescence from the active light-emitting layers which were fabricated as very dense thin films via vacuum deposition. This can offer the singlet emitters the opportunity to utilize the triplet excitons and thus actually raise the singlet to triplet exciton ratio in the non-doped OLEDs by using AIE-active materials with small $\triangle E_{ST}$ values.

Conclusions

In this work, four AIE molecules *o*-TPA-3TPE-*o*-PhCN, *o*-TPA-3TPE-*p*-PhCN, *p*-TPA-3TPE-*o*-PhCN and *p*-TPA-3TPE-

Physical Chemistry Chemical Physics Accepted Manuscript

This journal is © The Royal Society of Chemistry 2012

Table 1. Electroluminescent performances of D-3TPE-A molecules.[a]

Device	λ_{max} (nm)	V_{on} (V)	L_{max} (cd/m^2)	PE_{max} (lm/W)	CE_{max} (cd/A)	EQE_{max} (Experimental)	EQE_{max} (Theoretical)
o-TPA-3TPE-*o*-PhCN	444	5.3	146	2.3	2.7	1.72 %	1.2 %
o-TPA-3TPE-*p*-PhCN	516	5.6	1090	6.3	8.3	2.96 %	1.6 %
p-TPA-3TPE-*o*-PhCN	468	3.9	3790	4.2	4.8	2.93 %	2.0 %
p-TPA-3TPE-*p*-PhCN	512	4.4	36900	11.2	12.8	4.37 %	2.1 %

[a] Device configuration: ITO/NPB (60nm)/emitter (20nm)/TPBi (40nm)/LiF (1nm)/Al. Abbreviations: λ_{max} = EL maximum, V_{on} = turn-on voltage at 1 cd/m^2, L_{max} = maximum luminance, PE_{max} = maximum power efficiency, CE_{max} = maximum current efficiency, EQE_{max} = maximum external quantum efficiency, EQE_{max} (Theoretical) are calculated based on the singlet emitter-type device: the singlet/triplet exciton ratio is 1:3, and the out-coupling efficiency is 0.2 for the devices without optimizations.

p-PhCN were designed and synthesized towards fine tuning their $\triangle E_{ST}$ via HOMO-LUMO engineering and steric hindrance control. Interestingly, molecules with larger $\triangle E_{ST}$ values, such as *o*-TPA-3TPE-*o*-PhCN and *o*-TPA-3TPE-*p*-PhCN, can generate efficient low temperature long-lived phosphorescence with lifetime up to several seconds in their glassy solutions at 77 K. Meanwhile RTP can be readily achieved in their crystalline state. And for the first time, delay fluorescence is obtained in the crystals of *p*-TPA-3TPE-*p*-PhCN with a very small $\triangle E_{ST}$ value. Electroluminescent performance of these D-3TPE-A molecules were investigated as well, these devices showed high external quantum efficiency which were generally higher than their theoretical values on the general assumptions of singlet emitter-based devices. Particularly, *p*-TPA-3TPE-*p*-PhCN showed extraordinary EL performance with high luminance and efficiencies up to 36900 cd/m^2, 11.2 lm/W, 12.8 cd/A and 4.37%, respectively, considering that its solid-state quantum yield is only 42%.

Experimental

Materials and Synthesis

Tetrahydrofuran (THF, Labscan) were distilled in an atmosphere of dry nitrogen from sodium benzophenone ketyl immediately prior to use. 4-(diphenylamino)phenylboronic acid was synthesized according to literature method.[15] 2 and 4-bromobenzophenone, 2 and 4-bromobenzylbromide, triethylphosphite, 4-cyanophenylboronic acid, potassium *tert*-butodixe (*t*-BuOK) and other chemicals were purchased from Aldrich and used as received without further purification. Detailed synthetic procedures and characterizations are shown in Supporting Information.

Instrumentation

^{1}H and ^{13}C NMR spectra were measured on a Bruker ARX 400 NMR spectrometer using $CDCl_3$ (tetramethylsilane (TMS, $\delta = 0$) as internal reference) or DMSO-d_6 as deuterated solvent. MALDI-TOF spectra were recorded on a GCT Premier CAB048 mass spectrometer operating in a chemical ionization mode (CI) with methane as carrier gas. UV absorption spectra were taken on a Milton Ray Spectronic 3000 array spectrophotometer. Photoluminescenct (PL) spectra were recorded on a Perkin-Elmer LS 55 spectrofluorometer. Fluorescence decay curves were recorded on time-resolved fluorescence spectrometers.

Preparation of Aggregates

Stock THF solutions of D-3TPE-A molecules with a concentration of 0.1 mM were prepared. An aliquot (1 mL) of this stock solution was transferred to a 10 mL volumetric flask. After adding an appropriate amount of THF, water was added dropwise under vigorous stirring to furnish a 10 μM THF–water mixture with a specific water fraction. The water content was varied in the range of 0–95 vol%. Absorption and emission spectra of the resulting solutions and aggregates were measured immediately after the sample preparation.

Device fabrication

The devices were fabricated on 80 nm ITO-coated glass with a sheet resistance of 25 Ω/□. Prior to loading into the pretreatment chamber, the ITO-coated glasses were soaked in ultrasonic detergent for 30 min, followed by spraying with deionized water for 10 min, soaking in ultrasonic de-ionized water for 30 min, and oven-baking for 1 h. The cleaned samples were treated by perfluoromethane plasma with a power of 100 W, gas flow of 50 sccm, and pressure of 0.2 Torr for 10 s in the pretreatment chamber. The samples were transferred to the organic chamber with a base pressure of 7×10^{-7} Torr for the deposition of NPB, emitter, TPBi, and Alq_3. The samples were then transferred to the metal chamber for cathode deposition which composed of lithium fluoride (LiF) capped with aluminium (Al). The light-emitting area was 4 mm^2. The current density–voltage characteristics of the devices were measured by a HP4145B semiconductor parameter analyzer. The forward direction photons emitted from the devices were detected by a calibrated UDT PIN-25D silicon photodiode. The luminance and external quantum efficiencies of the devices were inferred from the photocurrent of the photodiode. The EL spectra were obtained by a PR650 spectrophotometer. All the measurements were carried out under air at room temperature without device encapsulation.

Acknowledgements

This work was partially supported by the National Basic Research Program of China (973 Program; 2013CB834701), the Research Grants Council of Hong Kong (604711, 602212, HKUST2/CRF/10, and N_HKUST620/11), the Innovation and Technology Commission (ITCPD/17-9), and the University Grants Committee of Hong Kong (AoE/P-03/08 and T23-713/11-1). B.Z.T. thanks the support from the Guangdong Innovative Research Team Program (201101C0105067115).

Physical Chemistry Chemical Physics Accepted Manuscript

Notes and references

[a] Department of Chemistry, Institute for Advanced Study, Division of Life Science, Institute of Molecular Functional Materials, Division of Biomedical Engineering and State Key Laboratory of Molecular Neuroscience, the Hong Kong University of Science and Technology (HKUST), Clear Water Bay, Kowloon, Hong Kong, China
[b] Department of Electronic and Computer Engineering, Center for Display Research, HKUST, Clear Water Bay, Kowloon, Hong Kong, China
[c] Department of Physics, HKUST, Clear Water Bay, Kowloon, Hong Kong, China
[d] HKUST Shenzhen Research Institute, No. 9 Yuexing 1st RD, South Area, High-tech Park, Nanshan, Shenzhen 518057, China.
[e] Guangdong Innovative Research Team, SCUT-HKUST Joint Research Laboratory, State Key Laboratory of Luminescent Materials and Devices, South China University of Technology, Guangzhou 510640, China

Electronic Supplementary Information (ESI) available, including structural characterization data and other supplementary photonic data. See DOI: 10.1039/b000000x/

1 *(a)* C. W. Tang and S. A. VanSlyke, *Appl. Phys. Lett,.* 1987, **51**, 913; (*b*) M. A. Baldo, D. F. O'Brien, Y. You, A. Shoustikov, S. Sibley, M. E. Thompson and S. R. Forrest, *Nature,* 1998, **395**, 151; (*c*) C. Adachi, M. A. Baldo, S. R. Forrest and M. E. Thompson, *Appl. Phys. Lett.,* 2000, **77**, 904; (*d*) Y. You, Y. Han, Y.-M. Lee, S. Y. Park, W. Nam and S. J. Lippard, *J. Am. Chem. Soc.,* 2011, **133**, 11488; (*e*) W. L. J. Rumsey, M. Vanderkooi and D. F. Wilson, *Science,* 1998, **241**, 1649; (*f*) J. G. J. E. D. Dolmans, D. Fukumura and R. K. Jain, *Nat. Rev. Cancer,* 2003, **3**, 380; (*g*) H. A. Collins, M. Khurana, E. H. Moriyama, A. Mariampillai, E. Dahlstedt, M. Balaz, M. K. Kuimova, M. Drobizhev, V. X. Yang, D. Phillips, A. Rebane, B. C. Wilson and H. L. Anderson, *Nat. Photonics,* 2008, **2**, 420; (*h*) J. W. Perry, K. Mansour, S. R. Marder, K. J. Perry, D. Alvarez and I. Choong, *Opt. Lett.,* 1994, **19**, 625; (*i*) G. J. Zhou, W. Y. Wong, S. Y. Poon, C. Ye and Z. Lin, *Adv. Funct. Mater.,* 2009, **19**, 531.

2 *(a)* S. Lamansky, P. Djurovich, D. Murphy, F. Abdel-Razzaq, H. Lee, C. Adachi, P. E. Burrows, S. R. Forrest and M. E. Thompson, *J. Am. Chem. Soc.,* 2001, **123**, 4304; (*b*) Y. Niu, Y. Tung, Y. Chi, C. Shu, J. H. Kim, B. Chen, J. Luo, A. J. Carty and A. K. Jen, *Chem. Mater.,* 2005, **17**, 3532; (*c*) C. Adachi, M. A. Baldo, M. E. Thompson and S. R. Forrest, *J. Appl. Phys.,* 2001, **90**, 5048; (*d*) L. Flamigni, A. Barbieri, C. Sabatini, B. Ventura and F. Barigelletti, *Top. Curr. Chem.,* 2007, **281**, 143; (*e*) A. J. G. Williams, *Top. Curr. Chem.,* 2007, **281**, 205.

3 *(a)* M. Montalti, A. Credi, L. Prodi and M. T. Gandol, *Handbook of Photochemistry*, *3rd edn*, Taylor & Francis: Boca Raton, USA 2006; (*b*) M. Kiritani, T. Yoshii, N. Hirota and M. Baba, *J. Chem. Phys.,* 1994, **98**, 11265; (*c*) D. R. Kearns and W. A. Case, *J. Am. Chem. Soc.,* 1966, **88**, 5087; (*d*) M. Klessinger and J. Michl, *Excited States and Photochemistry of Organic Molecules*, VCH Publishers: New York 1995.

4 W. Z. Yuan, X. Y. Shen, H. Zhao, J. W. Y. Lam, L. Tang, P. Lu, C. Wang, Y. Liu, Z. Wang, Q. Zheng, J. Z. Sun, Y. Ma and B. Z. Tang, *J. Phys. Chem. C,* 2010, **114**, 6090.

5 O. Bolton, K. Lee, H.-J. Kim, K. Y. Lin and J. Kim, *Nat. Chem.,* 2011, **3**, 205.

6 D. Lee, O. Bolton, B. C. Kim, J. H. Youk, S. Takayama and J. Kim, *J. Am. Chem. Soc.,* 2013, **135**, 6325.

7 S. Hirata, K. Totani, J. Zhang, T. Yamashita, H. Kaji, S. R. Marder, T. Watanabe and C. Adachi, *Adv. Funct. Mater.,* 2013, **23**, 3386.

8 *(a)* A. Endo, K. Sato, K. Yoshimura, T. Kai, A. Kawada, H. Miyazaki and C. Adachi, *Appl. Phys. Lett.,* 2011, **98**, 083302; (*b*) K. Goushi, K. Yoshida, K. Sato and C. Adachi, *Nat. Photonics,* 2012, **6**, 253; (*c*) T. Nakagawa, S.-Y. Ku, K.-T. Wong and C. Adachi, *Chem. Commun.,* 2012, **48**, 9580; (*d*) D. Y. Kondakov, T. D. Pawlik, T. K. Hatwar and J. P. Spindler, *J. Appl. Phys.,* 2009, **106**, 124510; (*e*) S. Y. Lee, T. Yasuda, H. Nomura and C. Adachi, *Appl. Phys. Lett.,* 2012, **101**, 093306; (*f*) G. Méhes, H. Nomura, Q. Zhang, T. Nakagawa and C. Adachi, *Angew. Chem. Int. Ed.,* 2012, **51**, 11311; (*g*) H. Tanaka, K. Shizu, H. Miyazaki and C. Adachi, *Chem. Commun.,* 2012, **48**, 11392; (*h*) Q. Zhang, J. Li, K. Shizu, S. Huang, S. Hirata, H. Miyazaki and C. Adachi, *J. Am. Chem. Soc.,* 2012, **134,** 14706; (*i*) H. Uoyama, K. Goushi, K. Shizu, H. Nomura and C Adachi, *Nature,* 2012, ***492***, 234.

9 (a) J. B.Birks, *Photophysics of Aromatic Molecules,* Wiley: London 1970; (*b*) J. Malkin, *Photophysical and Photochemical Properties of Aromatic Compounds*, CRC: Boca Raton 1992; (*c*) N. J. Turro, *Modern Molecular Photochemistry, University Science Books*, Mill Valley 1991.

10 *(a)* Y. Hong, J. W. Y. Lam and B. Z. Tang, *Chem. Commun.,* 2009, 4332; (*b*) Y. Hong, J. W. Y. Lam and B. Z. Tang, *Chem. Soc. Rev.,* 2011, **40**, 5361.

11 R. Hu, E. Lager, A. Aguilar-Aguilar, J. Liu, J. W. Y. Lam, H. H. Y. Sung, I. D. Williams, Y. Zhong, K. S. Wong, E. Peña-Cabrera and B. Z. Tang, *J. Phys. Chem. C,* 2009**, 113***,* 15845.

12 *(a)* W. Baumann, H. Bischof, J. C. Fröhling, C. Brittinger, W. Rettig and K. *J.* Rotkiewicz, *Photochem. Photobiol. A: Chem.,* 1992, **64**, 49; (*b*) Z. R. Grabowski and K. Rotkiewicz, *Chem. Rev.,* 2003, **103***,* 3899.

13 *(a)* J. Herbich, A. Kapturkiewicz and J. Nowacki, *Chem. Phys. Lett.,* 1996, **262**, 633; (*b*) Q. Zhang, J. Li, K. Shizu, S. Huang, S. Hirata, H. Miyazaki and C. Adachi, *J. Am. Chem. Soc.,* 2012, **134**, 14706; (c) F. B. Dias, K. N. Bourdakos, V. Jankus, K. C. Moss, K. T. Kamtekar, V. Bhalla, J. Santos and M. R. Bryce, A. P. Monkman, *Adv. Mater.,* 2013, **25**, 3707.

14 A. Köhler and H. Bässler, *Mater. Sci. Eng. R,* 2009, **66**, 71.

15 Z. Zhao, J. W. Y. Lam, C. Y. K. Chan, S. Chen, J. Liu, P. Lu, M. Rodriguez, J. –L. Maldonado, G. Ramos-Ortiz, H. H. Y. Sung, I. D. Williams, H. Su, K. S. Wong, Y. Ma, H. S. Kwok, H. Qiu and B. Z. Tang, *Adv. Mater.,* 2011, **23**, 5430.

Physical Chemistry Chemical Physics Accepted Manuscript

 This journal is © The Royal Society of Chemistry 2012